Dynamics and Control of an Octocopter with Flexible Structure

Danniel Stoller[1], Yoav Y. Biton[1], Shai Arogeti[2]
[1]Department of Mechanical Engineering, SCE, Shamoon College of Engineering, Beer Sheva, Israel
[2]Department of Mechanical Engineering, Ben-Gurion University of the Negev, Beer Sheva, Israel
dannist@ac.sce.ac.il, yoavybi@sce.ac.il, arogeti@bgu.ac.il

***Abstract*—This work introduces a multirotor aerial vehicle with a compliant structural framework, departing from the conventional rigid-body paradigm. Incorporating flexible members within the frame enables deformation modes that enhance disturbance rejection and maneuverability without auxiliary actuators. The inward orientation of rotor thrust vectors, achieved via compliant linkages, aligns reactive forces toward the center of mass and improves lateral perturbation resistance. Torsional compliance enables active yaw maneuvers without sole reliance on aerodynamic drag asymmetries. The system comprises four rotor pairs on flexible beams, yielding high actuation richness. A full nonlinear Euler–Lagrange model is derived analytically, and a PD controller with weighted pseudoinverse allocation is validated in simulation. Stable hover is achieved with RMS position error below 0.06 m, while a sustained 5 N wind disturbance reveals the limitations of the rigid-body PD/pseudoinverse controller and motivates future adaptive strategies. Enhanced dynamic performance and structural adaptability are demonstrated through geometric and material design alone, without increasing actuation complexity.**

Keywords: flexible multirotor, octocopter, compliant structure, Euler–Lagrange dynamics, PD control, pseudoinverse allocation, disturbance rejection.

I. Introduction

Multirotor aerial vehicles have seen rapid development, with applications spanning search and rescue, surveillance, and autonomous transportation [1]. Conventional platforms rely on rigid frames and fixed rotor geometries, which inherently limit independent control of all degrees of freedom (DoFs) and constrain disturbance rejection. Approaches based on tilted or reconfigurable rotors [1], [2] add actuation complexity. Omnidirectional designs [3] and seesaw-based octocopters [4], [5] represent related efforts; all rely on active mechanical components. This work instead proposes a compliant structural framework in which passive deformation enhances maneuverability and lateral disturbance resistance *without* additional actuators.

This work generalizes prior 10-DoF and 14-DoF flexible multirotor models (experimentally validated on a reduced-scale platform) into a scalable N-DoF framework. Following the rod-chain methodology of Biton [6], flexible arms are modeled as concatenations of rigid links connected by viscoelastic joints (Figure 1), each limited to a single DoF. Four such arms yield $4n$ structural DoFs alongside the rigid base. Net thrust drives arm bending for lateral translation; differential thrust drives torsion for yaw, decoupling translation from attitude without base reorientation.

The principal contributions of this work are:

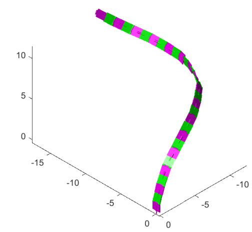

Fig. 1: A flexible rod of n rigid-link pairs enabling local bending and twisting. The nonlinear rigid–flexible equations of motion are derived from this representation.

- A scalable nonlinear Euler–Lagrange model for an octocopter with $4n$ flexible arm DoFs, derived fully analytically using a Jacobian-chain formulation.
- An alternating bending–torsion joint architecture that decouples lateral translation from base reorientation and enables active yaw without aerodynamic drag asymmetry.
- A modular PD control framework with weighted pseudoinverse rotor allocation that operates on aggregate arm states and is agnostic to the number of joints per arm, demonstrated here on a 46-DoF system ($n = 10$).

II. Structure, Kinematics, and Dynamics

A. Structure

The octocopter has eight rotors on four flexible arms. Each arm is a rod of n viscoelastic joints in alternating bending–torsion pairs: odd-indexed joints allow torsional deformation, even-indexed ones allow bending. Net thrust bends each arm to produce lateral translation; differential thrust between the two rotors on each arm twists it for yaw—permitting horizontal translation without base reorientation and significantly enhancing maneuverability.

III. Kinematics

Notation. $\boldsymbol{\xi} = [x, y, z]^T$ is the base center-of-mass position; ϕ, θ, ψ are roll, pitch, yaw; ϑ_i^k is the angle of joint i on arm $k \in \{a, b, c, d\}$; n (always even) is the number of joints per arm; $N = 6 + 4(n + 2)$ is the total DoF count; $\mathbf{q}$ is the configuration vector; $\mathbf{M}$, $\mathbf{V}$, $\mathbf{G}$, $\mathbf{Q}_{\text{gen}}$, $\mathbf{Q}_{\text{damp}}$ are the mass, Coriolis, gravity, actuator-force, and damping terms; G_1, G_2 and C_1, C_2 are bending/torsional stiffness (N·m/rad) and damping (N·m·s/rad); l_1–l_4 are link lengths (m); F_j^k, T_j^k are rotor thrust (N) and torque (N·m); κ_{thr} is the thrust coefficient.

In order to describe the drone's configuration in terms of both position and orientation, we define a fixed orthonormal triad (attached to an inertial frame) $\hat{e}1, \hat{e}2, \hat{e}3$ and a position vector $\boldsymbol{\xi} = x\hat{e}1 + y\hat{e}2 + z\hat{e}3$, representing the center of mass

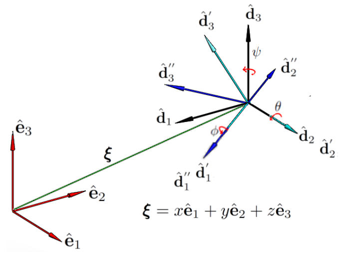

Fig. 2: A schematic description of the triads, the 3 position coordinates, x, y, z and the three angles ψ, θ, ϕ describing the position and orientation of the octocopter's base.

of the base, as illustrated in Figure 2. A rotation of the triad $\hat{\mathbf{e}}_1, \hat{\mathbf{e}}_2, \hat{\mathbf{e}}_3$ about $\hat{\mathbf{e}}_3$ by ψ aligns it with the triad $\hat{\mathbf{d}}_1, \hat{\mathbf{d}}_2, \hat{\mathbf{d}}_3$. Subsequently, a second rotation of $\hat{\mathbf{d}}_1, \hat{\mathbf{d}}_2, \hat{\mathbf{d}}_3$ about $\hat{\mathbf{d}}_2$ by θ results in the triad $\hat{\mathbf{d}}_1^{'}, \hat{\mathbf{d}}_2^{'}, \hat{\mathbf{d}}_3^{'}$. Finally, a third rotation of $\hat{\mathbf{d}}_1^{'}, \hat{\mathbf{d}}_2^{'}, \hat{\mathbf{d}}_3^{'}$ about $\hat{\mathbf{d}}_1^{'}$ yields the base orientation described by the triad $\hat{\mathbf{d}}_1^{''}, \hat{\mathbf{d}}_2^{''}, \hat{\mathbf{d}}_3^{''}$. Thus, the proper orthogonal transformation from components relative to the frame $\hat{\mathbf{d}}_1^{''}, \hat{\mathbf{d}}_2^{''}, \hat{\mathbf{d}}_3^{''}$, attached to the drone's base, to components in the inertial frame is given by:

$$
\begin{aligned}
{}^{\mathrm{I}}_{\mathrm{base}}\mathbf{R} &= \mathbf{R}_Z(\psi)\,\mathbf{R}_Y(\theta)\,\mathbf{R}_X(\phi) \\
&= \begin{bmatrix} \mathrm{c}_\theta \mathrm{c}_\psi & \mathrm{s}_\phi \mathrm{s}_\theta \mathrm{c}_\psi - \mathrm{c}_\phi \mathrm{s}_\psi & \mathrm{c}_\phi \mathrm{s}_\theta \mathrm{c}_\psi + \mathrm{s}_\phi \mathrm{s}_\psi \\ \mathrm{c}_\theta \mathrm{s}_\psi & \mathrm{s}_\phi \mathrm{s}_\theta \mathrm{s}_\psi + \mathrm{c}_\phi \mathrm{c}_\psi & \mathrm{c}_\phi \mathrm{s}_\theta \mathrm{s}_\psi - \mathrm{s}_\phi \mathrm{c}_\psi \\ -\mathrm{s}_\theta & \mathrm{s}_\phi \mathrm{c}_\theta & \mathrm{c}_\phi \mathrm{c}_\theta \end{bmatrix}
\end{aligned} \tag{1}
$$

where we use the abbreviations $\mathrm{s}_\varphi = \sin(\varphi)$ and $\mathrm{c}_\varphi = \cos(\varphi)$, and the matrices represent rotations about the X, Y, and Z axes.

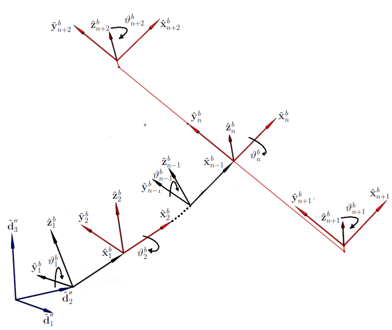

Fig. 3: Coordinate triads for the drone arms, showing position coordinates x, y, z and angles ψ, θ, ϕ. Each arm $k = a, b, c, d$ has its own triad rotated by $\alpha_k = 0, 90, 180, 270$ respectively.

The configuration of a simple drone is fully specified by $\boldsymbol{\xi}$ (i.e., x, y, z) and the three Euler angles ψ, θ, ϕ. Here, we present a drone with four flexible beams, each having n degrees of freedom (DoFs). Each beam consists of pairs of links with bending or twisting kinematics between consecutive links. Specifically, ϑ_i^k denotes the angle between any two links, where k represents one of the beams (a, b, c, d) and i denotes the link number within the beam. Angles ϑ_i^k with odd indices correspond to bending $({}^{\vartheta_{i-1}^k}_{\vartheta_i^k}R_y(\vartheta_i^k))$, while those with even indices correspond to twisting $({}^{\vartheta_{i-1}^k}_{\vartheta_i^k}R_x(\vartheta_i^k))$. Index n is always even. The rotation matrices of the rotors are rotational matrices around the $\hat{\mathbf{z}}$ $({}^{\vartheta_n^k}_{\vartheta_{n+j}^k}R_z(\vartheta_{n+j}^k))$,

The segment lengths l_1 (base to first joint), l_2 (between joints), l_3 (last joint to rotor beam), and l_4 (rotor offset) define the kinematic chain geometry used throughout the Jacobian derivations. A configuration is defined as the list of N DoFs specifying the spatial position and orientation of the system, where N is the sum of the DoFs for each beam, including two additional DoFs for the rotors on each beam, and the six DoFs of the base:

$$
\mathbf{q} = \begin{bmatrix} x & y & z & \phi & \theta & \psi & \vartheta_1^a & \cdots & \vartheta_{n+2}^d \end{bmatrix}^T \tag{2}
$$

We now need to designate an orthonormal triad to each of the arms. The choice we have made is as follows: (i) the x-axis direction, $\hat{\mathbf{x}}_{\alpha_j}$, is along the arm; (i) the y-axis direction, $\hat{\mathbf{y}}_{\alpha_j}$,of this system coincides with that of the associated joint, i.e., in the plane of the base and normal to the arm; (iii) the z-axis forms a right-handed orthonormal triad, as shown in Figure 3. Therefor, with the defined kinematics, we can systematically derive all the components of the unit vectors (given in terms of their components with respect to the inertial frame) of each of the arm-triads. The proper orthogonal transformations from components of a vector with respect to the triads $\{\hat{\mathbf{x}}_{\alpha_k}, \hat{\mathbf{y}}_{\alpha_k}, \hat{\mathbf{z}}_{\alpha_k},\}$, to its components with respect to the inertial frame are:

$$
{}^{\mathrm{I}}_{\alpha_k}\mathbf{R} = [{}^{\mathrm{I}}\hat{\mathbf{x}}_k,\, {}^{\mathrm{I}}\hat{\mathbf{y}}_k,\, {}^{\mathrm{I}}\hat{\mathbf{z}}_k] \tag{3}
$$

where the (3×1) columns ${}^{\mathrm{I}}\hat{\mathbf{x}}_k$, ${}^{\mathrm{I}}\hat{\mathbf{y}}_k$, and ${}^{\mathrm{I}}\hat{\mathbf{z}}_k$ are the components of $\hat{\mathbf{x}}_k$, $\hat{\mathbf{y}}_k$, and $\hat{\mathbf{z}}_k$ with respect to the inertial frame. The configuration space of the drone system is characterized by both the rigid body degrees of freedom and the flexible elements, which significantly impact the overall dynamics. We now proceed to derive the mathematical framework that captures this complex kinematic structure. The rotation of the first arm segment, as illustrated in Figure 3, occurs around the axis $\hat{\mathbf{y}}_{k_1}$, where α_k ($k = a, b, c,$ or d) represents a constant rotation around axis $\hat{\mathbf{d}}_3^{''}$. Specifically, $\alpha_a = 0$, $\alpha_b = 90°$, $\alpha_c = 180°$, and $\alpha_d = 270°$. When $\alpha_a = 0$ there is no rotation around axes $\hat{\mathbf{d}}_3^{''}$ and the new axis system is licked with the previous axis system. The rotation matrix respects to the base frame is define for ϑ_i^k ($k = a, b, c,$ or d) as, when i is odd the rotation matrix is around $\hat{\mathbf{y}}_i$ and represented as:

$$
{}^{\vartheta_{i-1}^k}_{\vartheta_i^k}R = \begin{bmatrix} c_{\vartheta_i^k} & 0 & s_{\vartheta_i^k} \\ 0 & 1 & 0 \\ -s_{\vartheta_i^k} & 0 & c_{\vartheta_i^k} \end{bmatrix}, \tag{4}
$$

while when i is even the rotation matrix is around $\hat{\mathbf{x}}_i$ and represented as:

$$
{}^{\vartheta_{i-1}^k}_{\vartheta_i^k}R = \begin{bmatrix} 1 & 0 & 0 \\ 0 & c_{\vartheta_i^k} & -s_{\vartheta_i^k} \\ 0 & s_{\vartheta_i^k} & c_{\vartheta_i^k} \end{bmatrix}, \tag{5}
$$

Index n is always even. The rotation matrices of the rotors are rotational matrices around the $\hat{\mathbf{z}}_{i+j}$ and represented as:

$$
{}^{\vartheta_n^k}_{\vartheta_{n+j}^k}R = \begin{bmatrix} c_{\vartheta_{n+j}^k} & -s_{\vartheta_{n+j}^k} & 0 \\ s_{\vartheta_{n+j}^k} & c_{\vartheta_{n+j}^k} & 0 \\ 0 & 0 & 1 \end{bmatrix}, \tag{6}
$$

where index j can be 1 or 2, 1 for the right rotor and 2 for the left one. The angular velocity vector of the base can be expressed in terms of its components with respect to the inertial frame as:

$$
\begin{aligned}
{}^{\mathrm{I}}\boldsymbol{\omega}_{\mathrm{base}} &= \begin{bmatrix} 0 \\ 0 \\ \dot{\psi} \end{bmatrix} + \mathbf{R}_Z(\psi) \begin{bmatrix} 0 \\ \dot{\theta} \\ 0 \end{bmatrix} \\
&+ \mathbf{R}_Z(\psi)\,\mathbf{R}_Y(\theta) \begin{bmatrix} \dot{\phi} \\ 0 \\ 0 \end{bmatrix} = \begin{bmatrix} \mathrm{c}_\psi \mathrm{c}_\theta \dot{\phi} - \mathrm{s}_\psi \dot{\theta} \\ \mathrm{c}_\psi \dot{\theta} + \mathrm{c}_\theta \mathrm{s}_\psi \dot{\phi} \\ \dot{\psi} - \mathrm{s}_\theta \dot{\phi} \end{bmatrix}.
\end{aligned} \tag{7}
$$

We construct a matrix composed of a chain of Jacobians, where each Jacobian is defined as a $3 \times N$ matrix. The first three rows are formulated as follows:

$$
{}^{\text{base}}\boldsymbol{\omega}_{\text{base}} = \begin{bmatrix} 1 & 0 & -s_\theta \\ 0 & c_\phi & c_\theta s_\phi \\ 0 & -s_\phi & c_\phi c_\theta \end{bmatrix} \tag{8}
$$

All other columns up to index N are zeros. The matrix $\mathbf{J}_{\text{base}}$ represents the derivative of ${}^{\mathrm{I}}\boldsymbol{\omega}_{\text{base}}$, as defined in equation 7, but expressed in the local frame.

The next four Jacobians, located below $\mathbf{J}_{\omega_{\text{base}}}$, are formulated as follows:

$$
\mathbf{J}_{\omega_{\vartheta_1^k}} = \left({}^{\mathrm{I}}_{\alpha^k}\mathbf{R}\,{}^{\alpha_k}_{\vartheta_1^k}\mathbf{R}\right)^T \mathbf{J}_{\omega_{\text{base}}} \tag{9}
$$

The subsequent column of these four Jacobians is $[0,1,0]^T$, representing the local rotation axis.

The next four Jacobians, located below $\mathbf{J}_{\omega_{\vartheta_1^k}}$, are defined as:

$$
\mathbf{J}_{\omega_{\vartheta_2^k}} = {}^{\vartheta_1^k}_{\vartheta_2^k}\mathbf{R}^T \mathbf{J}_{\omega_{\vartheta_1^k}} \tag{10}
$$

The subsequent column of these four Jacobians is $[1,0,0]^T$, representing the local rotation axis.

In general, each set of four Jacobians can be expressed as:

$$
\mathbf{J}_{\omega_{\vartheta_i^k}} = {}^{\vartheta_{i-1}^k}_{\vartheta_i^k}\mathbf{R}^T \mathbf{J}_{\omega_{\vartheta_{i-1}^k}} \tag{11}
$$

The subsequent column is $[0,1,0]^T$ when i is odd and $[1,0,0]^T$ when i is even. As stated earlier, n is always even.

The final eight Jacobians, corresponding to the rotors' angular velocities, are expressed as:

$$
\mathbf{J}_{\omega_{\vartheta_{n+j}^k}} = {}^{\vartheta_n^k}_{\vartheta_{n+j}^k}\mathbf{R}^T \mathbf{J}_{\omega_{\vartheta_n^k}} \tag{12}
$$

The subsequent row of these eight Jacobians is $[0,0,1]^T$.

Ultimately, a matrix of size $(3+3\cdot 4n+3\cdot 8)\times N$ is obtained. The first three rows correspond to $\mathbf{J}_{\omega_{\text{base}}}$, the next $3\cdot 4n$ rows correspond to $\mathbf{J}_{\omega_{\vartheta_i^k}}$, and the bottom rows correspond to the eight $\mathbf{J}_{\omega_{\vartheta_{n+j}^k}}$, where $j = 1$ refers to the right rotors, and $j = 2$ refers to the left rotors. This matrix is defined as $\mathbf{J}_\omega$.

Similar to angular velocity, the linear velocity is derived using a matrix constructed from a Jacobian chain, primarily based on $\mathbf{J}_\omega$. The first three rows form a 3×3 identity matrix:

$$
\mathbf{J}_{\boldsymbol{\xi}} = \begin{bmatrix} 1 & 0 & 0 \\ 0 & 1 & 0 \\ 0 & 0 & 1 \end{bmatrix} \tag{13}
$$

All other columns up to index N are zeros. The next four Jacobians are:

$$
\mathbf{J}_{\mathbf{v}_{\vartheta_1^k}} = \mathbf{J}_{\boldsymbol{\xi}} + {}^{\mathrm{I}}_{\vartheta_1^k}\mathbf{R} \begin{bmatrix} {}^{\alpha_1^k}\mathbf{r}_{\alpha_1^k,2}\cdot \mathbf{J}_{\omega_{\text{base},3}} - {}^{\alpha_1^k}\mathbf{r}_{\alpha_1^k,3}\cdot \mathbf{J}_{\omega_{\text{base},2}} \\ {}^{\alpha_1^k}\mathbf{r}_{\alpha_1^k,3}\cdot \mathbf{J}_{\omega_{\text{base},1}} - {}^{\alpha_1^k}\mathbf{r}_{\alpha_1^k,1}\cdot \mathbf{J}_{\omega_{\text{base},3}} \\ {}^{\alpha_1^k}\mathbf{r}_{\alpha_1^k,1}\cdot \mathbf{J}_{\omega_{\text{base},2}} - {}^{\alpha_1^k}\mathbf{r}_{\alpha_1^k,2}\cdot \mathbf{J}_{\omega_{\text{base},1}} \end{bmatrix}. \tag{14}
$$

where ${}^{\alpha_1^k}\mathbf{r}_{\alpha_1^k}$ is the distance from the center of the rigid base to each one of the first elastic joints.

$$
{}^{\alpha_1^k}\mathbf{r}_{\alpha_1^k} = [l_1, 0, 0]^T \tag{15}
$$

The subsequent Jacobians, continuing for all general coordinates up to index n, are defined as:

$$
\mathbf{J}_{\mathbf{v}_{\vartheta_i^k}} = \mathbf{J}_{\mathbf{v}_{\vartheta_{i-1}^k}} + {}^{\mathrm{I}}_{\vartheta_{i-1}^k}\mathbf{R} \begin{bmatrix} {}^{\vartheta_i^k}\mathbf{r}_{\vartheta_i^k,2}\cdot \mathbf{J}_{\omega_{\vartheta_{i-1}^k,3}} - {}^{\vartheta_i^k}\mathbf{r}_{\vartheta_i^k,3}\cdot \mathbf{J}_{\omega_{\vartheta_{i-1}^k,2}} \\ {}^{\vartheta_i^k}\mathbf{r}_{\vartheta_i^k,3}\cdot \mathbf{J}_{\omega_{\vartheta_{i-1}^k,1}} - {}^{\vartheta_i^k}\mathbf{r}_{\vartheta_i^k,1}\cdot \mathbf{J}_{\omega_{\vartheta_{i-1}^k,3}} \\ {}^{\vartheta_i^k}\mathbf{r}_{\vartheta_i^k,1}\cdot \mathbf{J}_{\omega_{\vartheta_{i-1}^k,2}} - {}^{\vartheta_i^k}\mathbf{r}_{\vartheta_i^k,2}\cdot \mathbf{J}_{\omega_{\vartheta_{i-1}^k,1}} \end{bmatrix}. \tag{16}
$$

where ${}^{\vartheta_i^k}\mathbf{r}_{\vartheta_i^k}$ is the distance from $i-1$ link to from i link.

$$
{}^{\vartheta_i^k}\mathbf{r}_{\vartheta_i^k} = [l_2, 0, 0]^T \tag{17}
$$

For the four Jacobians with index n, the formulation is similar, except for the distance vector:

$$
\mathbf{J}_{\mathbf{v}_{\vartheta_n^k}} = \mathbf{J}_{\mathbf{v}_{\vartheta_{n-1}^k}} + {}^{\mathrm{I}}_{\vartheta_{n-1}^k}\mathbf{R} \begin{bmatrix} {}^{\vartheta_n^k}\mathbf{r}_{\vartheta_n^k,2}\cdot \mathbf{J}_{\omega_{\vartheta_{n-1}^k,3}} - {}^{\vartheta_n^k}\mathbf{r}_{\vartheta_n^k,3}\cdot \mathbf{J}_{\omega_{\vartheta_{n-1}^k,2}} \\ {}^{\vartheta_n^k}\mathbf{r}_{\vartheta_n^k,3}\cdot \mathbf{J}_{\omega_{\vartheta_{n-1}^k,1}} - {}^{\vartheta_n^k}\mathbf{r}_{\vartheta_n^k,1}\cdot \mathbf{J}_{\omega_{\vartheta_{n-1}^k,3}} \\ {}^{\vartheta_n^k}\mathbf{r}_{\vartheta_n^k,1}\cdot \mathbf{J}_{\omega_{\vartheta_{n-1}^k,2}} - {}^{\vartheta_n^k}\mathbf{r}_{\vartheta_n^k,2}\cdot \mathbf{J}_{\omega_{\vartheta_{n-1}^k,1}} \end{bmatrix}. \tag{18}
$$

where ${}^{\vartheta_n^k}\mathbf{r}_{\vartheta_n^k}$ is the distance from $n-1$ link to from n link.

$$
{}^{\vartheta_n^k}\mathbf{r}_{\vartheta_n^k} = [l_3, 0, h_c]^T \tag{19}
$$

The final eight Jacobians, representing the linear velocities of the rotor centers of mass, do not depend on the angular velocities of the rotors and are defined as:

$$
\begin{aligned}
&\mathbf{J}_{\mathbf{v}_{\vartheta_n^k}} = \mathbf{J}_{\mathbf{v}_{\vartheta_{n-1}^k}} \\
&+ {}^{\mathrm{I}}_{\vartheta_{n-1}^k}\mathbf{R} \begin{bmatrix} {}^{\vartheta_n^k+j}\mathbf{r}_{\vartheta_n^k+j,2}\cdot \mathbf{J}_{\omega_{\vartheta_{n-1}^k,3}} - {}^{\vartheta_n^k+j}\mathbf{r}_{\vartheta_n^k+j,3}\cdot \mathbf{J}_{\omega_{\vartheta_{n-1}^k,2}} \\ {}^{\vartheta_n^k+j}\mathbf{r}_{\vartheta_n^k+j,3}\cdot \mathbf{J}_{\omega_{\vartheta_{n-1}^k,1}} - {}^{\vartheta_n^k+j}\mathbf{r}_{\vartheta_n^k+j,1}\cdot \mathbf{J}_{\omega_{\vartheta_{n-1}^k,3}} \\ {}^{\vartheta_n^k+j}\mathbf{r}_{\vartheta_n^k+j,1}\cdot \mathbf{J}_{\omega_{\vartheta_{n-1}^k,2}} - {}^{\vartheta_n^k+j}\mathbf{r}_{\vartheta_n^k+j,2}\cdot \mathbf{J}_{\omega_{\vartheta_{n-1}^k,1}} \end{bmatrix}
\end{aligned} \tag{20}
$$

where ${}^{\vartheta_{n+j}^k}\mathbf{r}_{\vartheta_{n+j}^k}$ is the distance from link n to the rotor (index $n+j$).

For the right rotor ($j = 1$):

$$
{}^{\vartheta_{n+1}^k}\mathbf{r}_{\vartheta_{n+1}^k} = [0, -l_4, 0]^T \tag{21}
$$

For the left rotor ($j = 2$):

$$
{}^{\vartheta_{n+2}^k}\mathbf{r}_{\vartheta_{n+2}^k} = [0, l_4, 0]^T \tag{22}
$$

Ultimately, a $\mathbf{J}_v$ matrix of size $(3+3\cdot 4n+3\cdot 8)\times N$ is obtained. The first three rows correspond to $\mathbf{J}_{\boldsymbol{\xi}}$, the next $3\cdot 4$ rows correspond to $\mathbf{J}_{v_{\vartheta_1^k}}$, the next $3\cdot 4(n-1)$ rows correspond to $\mathbf{J}_{v_{\vartheta_i^k}}$, and the bottom rows correspond to the eight $\mathbf{J}_{v_{\vartheta_{n+j}^k}}$, where $j = 1$ refers to the right rotors, and $j = 2$ refers to the left rotors.

The next step is to derivative $\mathbf{J}_\omega$ and $\mathbf{J}_v$ by each of the Dofs. To compute the derivatives of ${}^{\mathrm{I}}_{\text{base}}\mathbf{R}$ with respect to the Euler angles ϕ, θ, and ψ, we proceed as follows:

The derivatives of ${}^{\mathrm{I}}_{\text{base}}\mathbf{R}$ with respect to ϕ, θ, ψ follow from the product rule applied to the ZYX sequence: $\partial_\phi \mathbf{R} = \mathbf{R}_Z\mathbf{R}_Y(\partial_\phi \mathbf{R}_X)$, $\partial_\theta \mathbf{R} = \mathbf{R}_Z(\partial_\theta \mathbf{R}_Y)\mathbf{R}_X$, and $\partial_\psi \mathbf{R} = (\partial_\psi \mathbf{R}_Z)\mathbf{R}_Y\mathbf{R}_X$, where each single-axis derivative is the standard skew-symmetric form. Since $\mathbf{J}_\omega$ has no dependence on ψ, $\partial \mathbf{J}_{\omega_i}/\partial\psi = 0$ for all i.

We build a chain of matrices that are derivatives of $\mathbf{J}_\omega$ and $\mathbf{J}_v$. Since $\mathbf{J}_\omega$ does not depend on x, y, z

$$\frac{\partial \mathbf{J}_\omega}{\partial x} = \frac{\partial \mathbf{J}_\omega}{\partial y} = \frac{\partial \mathbf{J}_\omega}{\partial z} = 0 \tag{23}$$

The dependence of $\mathbf{J}_\omega$ on the degrees of freedom starts from ϕ The first three rows are formulated as follows:

$$\frac{\partial \mathbf{J}_{\omega_1}}{\partial \phi} = \begin{bmatrix} 0 & 0 & 0 \\ 0 & -s_\phi & c_\theta c_\phi \\ 0 & -c_\phi & -s_\phi c_\theta \end{bmatrix} \tag{24}$$

then,

$$\frac{\partial \mathbf{J}_{\omega_i}}{\partial \phi} = {}^{\vartheta^k_{i-1}}_{\vartheta^k_i} R^T \frac{\partial \mathbf{J}_{\omega_{i-1}}}{\partial \phi}. \tag{25}$$

The same operation we do for the second derivative, The first three rows are formulated as follows:

$$\frac{\partial \mathbf{J}_{\omega_1}}{\partial \theta} = \begin{bmatrix} 0 & 0 & -c_\theta \\ 0 & 0 & -s_\phi s_\theta \\ 0 & 0 & c_\phi s_\theta \end{bmatrix} \tag{26}$$

then,

$$\frac{\partial \mathbf{J}_{\omega_i}}{\partial \theta} = {}^{\vartheta^k_{i-1}}_{\vartheta^k_i} R^T \frac{\partial \mathbf{J}_{\omega_{i-1}}}{\partial \theta}. \tag{27}$$

Since $\mathbf{J}_\omega$ does not depend on ψ:

$$\frac{\partial \mathbf{J}_{\omega_1}}{\partial \psi} = 0 \tag{28}$$

and so are the all others $\frac{\partial \mathbf{J}_{\omega_i}}{\partial \psi} = 0$. From now on, the derivatives run on each beam separately, there is no dependence on the angular position of the base, the lines that do not depend on the Dof in which they are derived are zeroed:

$$\frac{\partial \mathbf{J}_{\omega_i}}{\partial \vartheta^k_p} = {}^{\vartheta^k_{i-1}}_{\vartheta^k_i} R^T \frac{\partial \mathbf{J}_{\omega_i}}{\partial \vartheta^k_{p-1}}. \tag{29}$$

where the index $i \geq p$.

Since $\mathbf{J}_v$ does not depend on x, y, z, the corresponding derivatives vanish. The first non-zero rows of $\frac{\partial \mathbf{J}_{\mathbf{v}_1}}{\partial \phi}$, beginning at row 4, are given by:

$$\frac{\partial \mathbf{J}_{v_{\vartheta^k_1}}}{\partial \phi} = \frac{\partial}{\partial \phi}\left({}^{\mathrm{I}}\boldsymbol{\omega}_{\mathrm{base}} \times {}^{\alpha^k_1}\mathbf{r}_{\alpha^k_1}\right) \tag{30}$$

The Jacobian derivative with respect to ϕ must account for both the change in the rotation matrix and the effect on the position vectors. This can be expressed as:

$$\begin{aligned}\frac{\partial \mathbf{J}_{v_{\vartheta^k_i}}}{\partial \phi} &= \frac{\partial \mathbf{J}_{v_{\vartheta^k_{i-1}}}}{\partial \phi} \\ &+ \frac{\partial\, {}^{\mathrm{I}}_{\mathrm{base}}\mathbf{R}}{\partial \phi}\, {}^{\mathrm{base}}_{\vartheta^k_i}\mathbf{R} \begin{bmatrix} {}^{\vartheta^k_i}\mathbf{r}_{\vartheta^k_i,2} \cdot \mathbf{J}_{\omega_{\vartheta^k_{i-1}},3} - {}^{\vartheta^k_i}\mathbf{r}_{\vartheta^k_i,3} \cdot \mathbf{J}_{\omega_{\vartheta^k_{i-1}},2} \\ {}^{\vartheta^k_i}\mathbf{r}_{\vartheta^k_i,3} \cdot \mathbf{J}_{\omega_{\vartheta^k_{i-1}},1} - {}^{\vartheta^k_i}\mathbf{r}_{\vartheta^k_i,1} \cdot \mathbf{J}_{\omega_{\vartheta^k_{i-1}},3} \\ {}^{\vartheta^k_i}\mathbf{r}_{\vartheta^k_i,1} \cdot \mathbf{J}_{\omega_{\vartheta^k_{i-1}},2} - {}^{\vartheta^k_i}\mathbf{r}_{\vartheta^k_i,2} \cdot \mathbf{J}_{\omega_{\vartheta^k_{i-1}},1} \end{bmatrix} \\ &+ {}^{\mathrm{I}}_{\vartheta^k_i}\mathbf{R} \begin{bmatrix} \frac{\partial\, {}^{\vartheta^k_i}\mathbf{r}_{\vartheta^k_i,2}}{\partial \phi} \cdot \mathbf{J}_{\omega_{\vartheta^k_{i-1}},3} - \frac{\partial\, {}^{\vartheta^k_i}\mathbf{r}_{\vartheta^k_i,3}}{\partial \phi} \cdot \mathbf{J}_{\omega_{\vartheta^k_{i-1}},2} \\ \frac{\partial\, {}^{\vartheta^k_i}\mathbf{r}_{\vartheta^k_i,3}}{\partial \phi} \cdot \mathbf{J}_{\omega_{\vartheta^k_{i-1}},1} - \frac{\partial\, {}^{\vartheta^k_i}\mathbf{r}_{\vartheta^k_i,1}}{\partial \phi} \cdot \mathbf{J}_{\omega_{\vartheta^k_{i-1}},3} \\ \frac{\partial\, {}^{\vartheta^k_i}\mathbf{r}_{\vartheta^k_i,1}}{\partial \phi} \cdot \mathbf{J}_{\omega_{\vartheta^k_{i-1}},2} - \frac{\partial\, {}^{\vartheta^k_i}\mathbf{r}_{\vartheta^k_i,2}}{\partial \phi} \cdot \mathbf{J}_{\omega_{\vartheta^k_{i-1}},1} \end{bmatrix}\end{aligned} \tag{31}$$

Similarly, the following derivative can be obtained:

$$\frac{\partial \mathbf{J}_{v_{\vartheta^k_1}}}{\partial \theta} = \frac{\partial}{\partial \theta}\left({}^{\mathrm{I}}\boldsymbol{\omega}_{\mathrm{base}} \times {}^{\alpha^k_1}\mathbf{r}_{\alpha^k_1}\right) \tag{32}$$

then,

$$\begin{aligned}\frac{\partial \mathbf{J}_{v_{\vartheta^k_i}}}{\partial \theta} &= \frac{\partial \mathbf{J}_{v_{\vartheta^k_{i-1}}}}{\partial \theta} \\ &+ \frac{\partial\, {}^{\mathrm{I}}_{\mathrm{base}}\mathbf{R}}{\partial \theta}\, {}^{\mathrm{base}}_{\vartheta^k_i}\mathbf{R} \begin{bmatrix} {}^{\vartheta^k_i}\mathbf{r}_{\vartheta^k_i,2} \cdot \mathbf{J}_{\omega_{\vartheta^k_{i-1}},3} - {}^{\vartheta^k_i}\mathbf{r}_{\vartheta^k_i,3} \cdot \mathbf{J}_{\omega_{\vartheta^k_{i-1}},2} \\ {}^{\vartheta^k_i}\mathbf{r}_{\vartheta^k_i,3} \cdot \mathbf{J}_{\omega_{\vartheta^k_{i-1}},1} - {}^{\vartheta^k_i}\mathbf{r}_{\vartheta^k_i,1} \cdot \mathbf{J}_{\omega_{\vartheta^k_{i-1}},3} \\ {}^{\vartheta^k_i}\mathbf{r}_{\vartheta^k_i,1} \cdot \mathbf{J}_{\omega_{\vartheta^k_{i-1}},2} - {}^{\vartheta^k_i}\mathbf{r}_{\vartheta^k_i,2} \cdot \mathbf{J}_{\omega_{\vartheta^k_{i-1}},1} \end{bmatrix} \\ &+ {}^{\mathrm{I}}_{\vartheta^k_i}\mathbf{R} \begin{bmatrix} \frac{\partial\, {}^{\vartheta^k_i}\mathbf{r}_{\vartheta^k_i,2}}{\partial \theta} \cdot \mathbf{J}_{\omega_{\vartheta^k_{i-1}},3} - \frac{\partial\, {}^{\vartheta^k_i}\mathbf{r}_{\vartheta^k_i,3}}{\partial \theta} \cdot \mathbf{J}_{\omega_{\vartheta^k_{i-1}},2} \\ \frac{\partial\, {}^{\vartheta^k_i}\mathbf{r}_{\vartheta^k_i,3}}{\partial \theta} \cdot \mathbf{J}_{\omega_{\vartheta^k_{i-1}},1} - \frac{\partial\, {}^{\vartheta^k_i}\mathbf{r}_{\vartheta^k_i,1}}{\partial \theta} \cdot \mathbf{J}_{\omega_{\vartheta^k_{i-1}},3} \\ \frac{\partial\, {}^{\vartheta^k_i}\mathbf{r}_{\vartheta^k_i,1}}{\partial \theta} \cdot \mathbf{J}_{\omega_{\vartheta^k_{i-1}},2} - \frac{\partial\, {}^{\vartheta^k_i}\mathbf{r}_{\vartheta^k_i,2}}{\partial \theta} \cdot \mathbf{J}_{\omega_{\vartheta^k_{i-1}},1} \end{bmatrix}\end{aligned} \tag{33}$$

and the derivative by ψ:

$$\frac{\partial \mathbf{J}_{v_{\vartheta^k_1}}}{\partial \psi} = \frac{\partial}{\partial \psi}\left({}^{\mathrm{I}}\boldsymbol{\omega}_{\mathrm{base}} \times {}^{\alpha^k_1}\mathbf{r}_{\alpha^k_1}\right) \tag{34}$$

then,

$$\frac{\partial \mathbf{J}_{v_{\vartheta^k_i}}}{\partial \psi} = \frac{\partial \mathbf{J}_{v_{\vartheta^k_{i-1}}}}{\partial \psi} + \frac{\partial\, {}^{\mathrm{I}}_{\mathrm{base}}\mathbf{R}}{\partial \psi} \begin{bmatrix} {}^{\vartheta^k_i}\mathbf{r}_{\vartheta^k_i,2} \cdot \mathbf{J}_{\omega_{\vartheta^k_{i-1}},3} - {}^{\vartheta^k_i}\mathbf{r}_{\vartheta^k_i,3} \cdot \mathbf{J}_{\omega_{\vartheta^k_{i-1}},2} \\ {}^{\vartheta^k_i}\mathbf{r}_{\vartheta^k_i,3} \cdot \mathbf{J}_{\omega_{\vartheta^k_{i-1}},1} - {}^{\vartheta^k_i}\mathbf{r}_{\vartheta^k_i,1} \cdot \mathbf{J}_{\omega_{\vartheta^k_{i-1}},3} \\ {}^{\vartheta^k_i}\mathbf{r}_{\vartheta^k_i,1} \cdot \mathbf{J}_{\omega_{\vartheta^k_{i-1}},2} - {}^{\vartheta^k_i}\mathbf{r}_{\vartheta^k_i,2} \cdot \mathbf{J}_{\omega_{\vartheta^k_{i-1}},1} \end{bmatrix} \tag{35}$$

the difference between equation 35 and 31-33 because $\frac{\partial \mathbf{J}_{\omega_i}}{\partial \psi} = 0$. Let us note that the derivatives of the Jacobian matrices that return the velocities of the four bending axes were computed analytically directly from the expressions representing their positions. The remaining derivatives were also obtained analytically by properly calculating the derivatives of the product of orthogonal transformations (see Equation 31,33 and 35). The same approach can be followed for each subsequent Dofs for derivatives with respect to other generalized coordinates. For the general case of derivatives with respect to joint angles ϑ^k_P, we must consider how changes in these angles affect both the rotation matrices and the position vectors of subsequent links in the kinematic chain:

$$\begin{aligned}\frac{\partial \mathbf{J}_{v_{\vartheta^k_i}}}{\partial \vartheta^k_P} &= \frac{\partial \mathbf{J}_{v_{\vartheta^k_{i-1}}}}{\partial \vartheta^k_P} + {}^{\mathrm{I}}_{\vartheta^k_{i-1}}\mathbf{R} \frac{\partial\, {}^{\vartheta^k_{i-1}}_{\vartheta^k_i}\mathbf{R}}{\partial \vartheta^k_P}\, {}^{\vartheta^k_{i-1}}_{\vartheta^k_i}\mathbf{R}^{\mathrm{T}}\, {}^{\vartheta^k_i}_{\vartheta^k_{i+1}}\mathbf{R} \\ &\quad \begin{bmatrix} {}^{\vartheta^k_i}\mathbf{r}_{\vartheta^k_i,2} \cdot \mathbf{J}_{\omega_{\vartheta^k_{i-1}},3} - {}^{\vartheta^k_i}\mathbf{r}_{\vartheta^k_i,3} \cdot \mathbf{J}_{\omega_{\vartheta^k_{i-1}},2} \\ {}^{\vartheta^k_i}\mathbf{r}_{\vartheta^k_i,3} \cdot \mathbf{J}_{\omega_{\vartheta^k_{i-1}},1} - {}^{\vartheta^k_i}\mathbf{r}_{\vartheta^k_i,1} \cdot \mathbf{J}_{\omega_{\vartheta^k_{i-1}},3} \\ {}^{\vartheta^k_i}\mathbf{r}_{\vartheta^k_i,1} \cdot \mathbf{J}_{\omega_{\vartheta^k_{i-1}},2} - {}^{\vartheta^k_i}\mathbf{r}_{\vartheta^k_i,2} \cdot \mathbf{J}_{\omega_{\vartheta^k_{i-1}},1} \end{bmatrix} \\ &+ {}^{\mathrm{I}}_{\vartheta^k_i}\mathbf{R} \begin{bmatrix} \frac{\partial\, {}^{\vartheta^k_i}\mathbf{r}_{\vartheta^k_i,2}}{\partial \vartheta^k_P} \cdot \mathbf{J}_{\omega_{\vartheta^k_{i-1}},3} - \frac{\partial\, {}^{\vartheta^k_i}\mathbf{r}_{\vartheta^k_i,3}}{\partial \vartheta^k_P} \cdot \mathbf{J}_{\omega_{\vartheta^k_{i-1}},2} \\ \frac{\partial\, {}^{\vartheta^k_i}\mathbf{r}_{\vartheta^k_i,3}}{\partial \vartheta^k_P} \cdot \mathbf{J}_{\omega_{\vartheta^k_{i-1}},1} - \frac{\partial\, {}^{\vartheta^k_i}\mathbf{r}_{\vartheta^k_i,1}}{\partial \vartheta^k_P} \cdot \mathbf{J}_{\omega_{\vartheta^k_{i-1}},3} \\ \frac{\partial\, {}^{\vartheta^k_i}\mathbf{r}_{\vartheta^k_i,1}}{\partial \vartheta^k_P} \cdot \mathbf{J}_{\omega_{\vartheta^k_{i-1}},2} - \frac{\partial\, {}^{\vartheta^k_i}\mathbf{r}_{\vartheta^k_i,2}}{\partial \vartheta^k_P} \cdot \mathbf{J}_{\omega_{\vartheta^k_{i-1}},1} \end{bmatrix}\end{aligned} \tag{36}$$

IV. DYNAMICS BASED ON THE EULER-LAGRANGE FORMULATION

The dynamics are derived using the Euler-Lagrange approach, incorporating the interactions between the rigid base, flexible arms, and rotor dynamics, with both conservative and non-conservative forces.

We define the non-conservative forces as a combination of the moments produced by the eight motors and the lift forces of the eight rotors produced by their angular velocities. For the relationship between thrust, torque, and the angular velocity of each rotor, we use:

$$F_j^k = \kappa_{\text{thr}} \left(\dot{\vartheta}_{n+j}^k\right)^2,, \;\; T_j^k = \mathbf{I}_{n+j}^k \ddot{\vartheta}_{n+j}^k \tag{37}$$

where κ_{thr} is the thrust coefficient, with $\dot{\vartheta}_{n+j}^k = 8000$ RPM generating approximately 10 N of thrust and 0.1 Nm of torque. The term $\mathbf{I}_{n+j}^k$ represents the moment of inertia of each rotor with its motor, and $\ddot{\vartheta}_{n+j}^k$ is the angular acceleration of the corresponding rotor.

To express the influence of these non-conservative forces, we define appropriate Jacobians for each force and moment from equation 37. The Jacobian $\mathbf{J}_{F_j^k}$ is defined as the partial derivative of the velocity vectors with respect to the generalized coordinates $\dot{\mathbf{q}}_i$. This Jacobian is represented as a $3 \times N$ matrix:

$$\mathbf{J}_{F_j^k} = \mathbf{J}_{v_{\vartheta_{n+j}^k}} \tag{38}$$

Similarly, the Jacobians for each moment from equation 37 are defined as:

$$\mathbf{J}_{T_j^k} = \mathbf{J}_{\omega_{\vartheta_{n+j}^k}} \tag{39}$$

The virtual work for these non-conservative forces is then formulated as:

$$\delta \mathbf{W}_{\mathbf{F}_j^k} = \delta \mathbf{q}^T \mathbf{J}_{F_j^k}^T \, {}^{\mathrm{I}}_{\vartheta_{n+j}^k}\mathbf{R}[\mathbf{0}, \mathbf{0}, F_j^k]^T, \;\; \delta \mathbf{W}_{\mathbf{T}_j^k} = \delta \mathbf{q}^T \mathbf{J}_{\boldsymbol{\omega}_{\vartheta_{n+j}^k}}^T [\mathbf{0}, \mathbf{0}, T_j^k]^T, \tag{40}$$

where $\delta \mathbf{W}_{\mathbf{F}_j^k}$ represents the virtual work of $\mathbf{F}_j^k$ and $\delta \mathbf{W}_{\mathbf{T}_j^k}$ is the virtual work of $\mathbf{T}_j^k$.

It is important to note that the linear velocities are defined in the inertial frame, while the forces $\mathbf{F}_j^k$ act in the $\hat{\mathbf{z}}_{n+j}^k$ direction (as depicted in Figure 2). Therefore, the force $\mathbf{F}_j^k$ must be transformed to the inertial frame using the rotation matrix ${}^{\mathrm{I}}_{\vartheta_{n+j}^k}\mathbf{R}$. The angular velocities are defined in the local frames, and consequently, the torque T_j^k acts in the $\hat{\mathbf{z}}_{n+j}^k$ direction. Specifically, the torques $\mathbf{T}_1^k$ around $\hat{\mathbf{z}}_1^k$ operate clockwise, while the torques $\mathbf{T}_2^k$ around $\hat{\mathbf{z}}_2^k$ operate counterclockwise.

The total virtual work is the sum of all contributions:

$$\delta \mathbf{W}_{tot} = \sum_{k=a,b,c,d, j=1,2} \delta \mathbf{W}_{\mathbf{F}_j^k} + \sum_{k=a,b,c,d, j=1,2} \delta \mathbf{W}_{\mathbf{T}_j^k} \tag{41}$$

The generalized force vector $\mathbf{Q}_{gen}$ is defined as the sum of all forces and moments acting on the system, multiplied by the appropriate Jacobians:

$$\mathbf{Q}_{gen} = \sum_{k=a,b,c,d, j=1,2} \left(\mathbf{J}_{F_j^k}^{\mathbf{T}} \, {}^{\mathrm{I}}_{\vartheta_{n+j}^k}\mathbf{R}[\mathbf{0}, \mathbf{0}, F_j^k]^{\mathbf{T}} + \mathbf{J}_{\boldsymbol{\omega}_{\vartheta_{n+j}^k}} [\mathbf{0}, \mathbf{0}, T_j^k]^{\mathbf{T}} \right), \tag{42}$$

Each viscoelastic joint also experiences damping about its local rotation axis, alternating between $\hat{\mathbf{y}}$ (odd joints) and $\hat{\mathbf{x}}$ (even joints), linearly proportional to $\dot{\vartheta}_i^k$. The damping vector is formulated as:

$$\mathbf{Q}_{\text{damp}} = \left[\mathbf{0}, \mathbf{0}, \mathbf{0}, \mathbf{0}, \mathbf{0}, \mathbf{0}, C_{\vartheta_1^a}, ..., C_{\vartheta_n^d}, 0, 0, 0, 0, 0, 0, 0, 0\right]^T \dot{\mathbf{q}} \tag{43}$$

where $\mathbf{Q}_{damp}$ is an $N \times 1$ vector with the same dimensions as $\mathbf{q}$. Note that there are no viscoelastic joints in the first 6 DoFs (which correspond to the rigid base) and the last 8 DoFs (which correspond to the rotors).

To systematically derive the equations of motion, we employ the Euler-Lagrange formulation. The mass matrix $\mathbf{M}$ is constructed as the sum of contributions from the linear and angular motion of each link:

$$\mathbf{M} = \sum_{i=1}^{N} \left(\mathbf{J}_{v_{\vartheta_i^k}}^T \mathbf{m}_{\vartheta_i^k} \mathbf{J}_{v_{\vartheta_i^k}} + \mathbf{J}_{\omega_{\vartheta_i^k}}^T \mathbf{I}_{\vartheta_i^k} \mathbf{J}_{\omega_{\vartheta_i^k}} \right) \tag{44}$$

where $\mathbf{m}_{\vartheta_i^k}$ and $\mathbf{I}_{\vartheta_i^k}$ are the mass and inertia matrix of link i.

The nonlinear terms $\mathbf{V}(\dot{\mathbf{q}}, \mathbf{q})$ account for Coriolis and centrifugal effects, and are composed of two components:

$$\mathbf{V}_{\text{tot}} = \mathbf{V}_1 + \mathbf{V}_2 \tag{45}$$

The first component $\mathbf{V}_1$ captures the rate of change of the mass matrix with respect to the generalized coordinates:

$$\mathbf{V}_1 = \sum_{i=1}^{N} \left(\frac{\partial \mathbf{M}}{\partial q_i} \dot{q}_i \right) \dot{\mathbf{q}} \tag{46}$$

The second component $\mathbf{V}_2$ accounts for the coupling between velocity and configuration-dependent mass properties:

$$\mathbf{V}_2 = -\frac{1}{2} \left[\dot{\mathbf{q}}^T \frac{\partial \mathbf{M}}{\partial q_1} \dot{\mathbf{q}}, \; \dot{\mathbf{q}}^T \frac{\partial \mathbf{M}}{\partial q_2} \dot{\mathbf{q}}, \; \cdots, \; \dot{\mathbf{q}}^T \frac{\partial \mathbf{M}}{\partial q_N} \dot{\mathbf{q}} \right]^T \tag{47}$$

The potential energy u consists of two components: gravitational potential energy u_1 and elastic potential energy u_2:

$$u_1 = \sum_{i=1}^{N} m_{\vartheta_i^k} g \mathbf{r}_{\vartheta_i^k} \hat{\mathbf{e}}_3 \tag{48}$$

where the index 3 refers to the z component of the location vector $\mathbf{r}_{\vartheta_i^k}$ in the inertial frame.

The elastic potential energy is formulated as:

$$u_2 = 0.5G \sum_{i=1, k=a,b,c,d}^{n} {\vartheta_i^k}^2 \tag{49}$$

where G is the elasticity coefficient, which differs between bending links (G_1) and twisting links (G_2).

The generalized gravitational forces $\mathbf{G}$ are defined as the partial derivative of the potential energy U:

$$\mathbf{G} = \left[\frac{\partial U}{\partial q_1}, \frac{\partial u}{\partial q_2}, \cdots, \frac{\partial u}{\partial q_N} \right]^T \tag{50}$$

The derivative of u_1 with respect to q_i is:

$$\frac{\partial u_1}{\partial q_i} = \left[m_{base} g \mathbf{J}_{\dot{\boldsymbol{\xi}},3}, m_{\vartheta_1^1} g \mathbf{J}_{v_{\vartheta_1^1},3}, \cdots, m_{\vartheta_{n+2}^4,3} g \mathbf{J}_{v_{\vartheta_{n+2}^4},3} \right]^T \tag{51}$$

which incorporates the z components of the Jacobians from equations 13-36.

The derivative of u_2 with respect to q_i is:

$$\frac{\partial u_2}{\partial q_i} = \left[0, 0, 0, 0, 0, 0, G_{\vartheta_1^a}, ..., G_{\vartheta_n^d}, 0, 0, 0, 0, 0, 0, 0, 0\right]^T \mathbf{q} \tag{52}$$

From all the above formulations, the complete equations of motion can be expressed in the standard form:

$$\mathbf{M}\ddot{\mathbf{q}} + \mathbf{V}(\dot{\mathbf{q}}, \mathbf{q}) + \mathbf{G}(\mathbf{q}) = \mathbf{Q}_{\text{gen}}(\mathbf{q}) - \mathbf{Q}_{\text{damp}}(\mathbf{q}) \tag{53}$$

where $\mathbf{M}$, $\mathbf{V}$, $\mathbf{G}$, $\mathbf{Q}_{\text{gen}}$, $\mathbf{Q}_{\text{damp}}$ are the mass matrix, Coriolis/centrifugal, gravitational, generalized force, and damping vectors respectively.

Equation 53 can be rearranged to express the accelerations explicitly:

$$\ddot{\mathbf{q}} = \mathbf{M}^{-1}\left[-\mathbf{V} - \mathbf{G} - \mathbf{Q}_{\text{damp}} + \mathbf{Q}_{\text{gen}}\right] \tag{54}$$

V. Control System Implementation and Results

A PD control system with weighted pseudoinverse rotor allocation was implemented, targeting hover at $[2, 1, 1]^T$. A PD law computes desired forces and moments $\mathbf{u} = [F_x, F_y, F_z, \mathbf{M}_{xy}, M_\psi]^T$; these are mapped to rotor speeds via $\mathbf{\Omega} = W_E P^T (P W_E P^T)^{-1}\mathbf{u}$, where $W_E = \text{diag}(w_1, \ldots, w_8)$ distributes effort to minimize structural excitation. The controller acts on the six rigid-body DoFs; flexible and rotor DoFs are treated as internal states. Simulation parameters are in Table I; all runs used $n = 2$ ($N = 22$ DoFs).

TABLE I: Simulation Parameters

Parameter	Value	Unit
m_{base} / m_{link} / m_{tip} / m_{rotor}	0.1 / 0.025 / 0.1 / 0.05	kg
l_1 / l_2	0.1 / 0.05	m
$I_{base_{xx,yy}}$ / $I_{base_{zz}}$	0.00075 / 0.0015	kg·m^2
G_1 / G_2	20 / 70	N·m
C_1 / C_2	3 / 2	N·m·s
κ_{thr} / k_t/k_f	0.12 / 0.01	–

Hover test. Figure 4 shows the resulting trajectory, confirming stable hover convergence. The RMS position error in x and y is below 0.04 m; altitude (z) settles within approximately 2 s with a peak overshoot of 0.12 m and a steady-state RMS of 0.06 m, attributable to flexible-arm coupling.

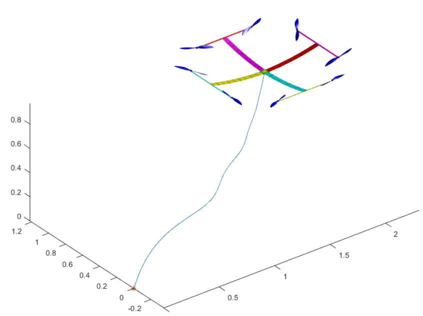

Fig. 4: Hover test: drone commanded to $[2, 1, 1]^T$. Trajectory converges; residual altitude oscillation reflects rigid–flexible coupling (RMS z-error = 0.06 m, settling time ≈ 2 s).

Wind-disturbance test. A sustained 5 N horizontal load was applied in the negative $\hat{e}_2$ direction, simulating moderate wind. As shown in Figure 5, the y-axis deviation reaches a peak of 0.31 m and the altitude error grows to an RMS of 0.19 m, exposing the limitations of the rigid-body PD controller in the presence of structural flexibility.

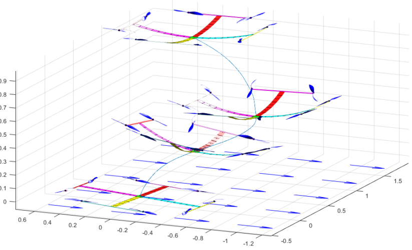

Fig. 5: Wind-disturbance test: 5 N horizontal load in $-\hat{e}_2$. Peak lateral deviation 0.31 m; altitude RMS error 0.19 m vs. 0.06 m in hover, highlighting the need for flexibility-aware control.

The hover results validate the N-DoF modeling framework and confirm that the PD/pseudoinverse controller, tuned on rigid-body states alone, achieves stable equilibrium. The wind-disturbance scenario reveals that the RMS altitude error triples and the lateral error quadruples relative to hover, underscoring the need for controllers that explicitly account for arm flexibility. These findings motivate future work on adaptive and learning-based control strategies. While experimental hardware validation remains an important next step, the current results establish a quantitative baseline for flexible multirotor control.

VI. Conclusions

Three principal contributions were made: (i) a scalable Euler–Lagrange model with $4n$ flexible DoFs derived analytically via a Jacobian-chain formulation; (ii) an alternating bending–torsion joint architecture decoupling translation from base attitude; and (iii) a modular PD/pseudoinverse framework validated on a 46-DoF system. Stable hover converged to $[2, 1, 1]^T$; a 5 N wind disturbance caused substantially larger deviations, identifying the limits of the rigid-body PD controller. These findings are consistent with earlier experimental results on a 14-DoF platform, where flexibility attenuated oscillatory response relative to a rigid baseline. Future work targets flexibility-aware adaptive control, hardware prototyping, and the strain-gauge-based arm-state estimator developed in related work.

References

[1] E. Hanoch, A. Shapiro, and G. Weiss, "Quadrotor with a dihedral angle: on the effects of tilting the rotors inwards," *J. Intell. Robot. Syst.*, vol. 80, no. 2, pp. 313–324, 2015.

[2] M. Elfeky, M. Elshafei, A.-W. A. Saif, and M. F. Al-Malki, "Quadrotor helicopter with tilting rotors: Modeling and simulation," in *Proc. WCCIT*, 2013, pp. 1–5.

[3] P. Shu, F. Li, J. Zhao, and M. Oya, "Robust adaptive control for a novel fully-actuated octocopter UAV with wind disturbance," *J. Intell. Robot. Syst.*, vol. 103, pp. 1–17, 2021.

[4] D. Yecheskel and S. Arogeti, "Modeling and control of a hexacopter with a rotating seesaw," in *Proc. ICARCV*, 2016, pp. 1–6.

[5] D. Yecheskel and S. Arogeti, "A fully-actuated drone with rotating seesaws," in *Proc. ICUAS*, 2023, pp. 1114–1121.

[6] Y. Y. Biton, B. D. Coleman, and D. Swigon, "Bifurcations of equilibria of intrinsically curved rod-like structures," *J. Elasticity*, vol. 87, no. 2, pp. 187–210, 2007.